

INTERACTIVE DETECTION OF 3D MODELS OF BUILDING'S ROOFING FOR THE ESTIMATION OF THE SOLAR ENERGY POTENTIAL

S. Brofferio¹, D. Passoni, M.E. Gaetani², M. Spertino³,

¹ Politecnico di Milano: DEI
 Piazza L. da Vinci 32, 20133 Milano, Italy
 phone: +39 02 23993577, email: sergio.brofferio@polimi.it

² Politecnico di Milano: DIAR
 Piazza L. da Vinci 32, 20133 Milano, Italy
 phone: +39 02 23996525, email: daniele.passoni@polimi.it

³ CNR Torino IEIIT
 C.so Duca degli Abruzzi 24, 10129 Torino, Italy
 phone: +39 011 3919247, email: spertino@iriti.cnr.it

ABSTRACT

The paper presents the work in progress of the design and implementation of an interactive system for the detection of the building's roofing characteristic. For each of its pitches data concerning height, shape, orientation, slope and useful area are estimated at different precision levels. The system operates on a cartographic map and two pre-processed aerial photographs that are aligned for building selection, image segmentation and 3D modelling. Each building roofing is automatically classified and its features are used for disparity computation from two stereoscopic views for precise 3D modelling. Different disparity measurement algorithms are being experimented to measure their accuracy based on reference test buildings. The 3D model is the input to standard software packages for solar energy potential estimation

1. INTRODUCTION

Solar energy is an increasing complementary energy source in view of limiting and reducing the need of non renewable and polluting energy resources. The estimation of the solar energy potential of building roofing is an important first step for the Building Integrated Photovoltaic (BIPV) and thermal solar energy exploitation [1].

This potential has to be evaluated at the building scale to be of real help to local policy makers and for system design. Building heights, roofing orientations, slopes and useful areas are the input to solar radiation application software [2] and shadows cones evaluation programs. It should be noted that requirements on the accuracy of shadow cones are more strict than the ones for modules radiation and depend on the inter-building distances and heights.

This research concerns the study, design and implementation of an interactive software tool for the construction of a 3D model of the building with an accuracy of at least 50 cm so that the essential roofing parameters can be computed [3], [4]. The input data are:

- 1) a cartographic map at a scale of 1:2000 (or better) that show, at least, building imprint and the Ground Numerical Model (GNM). The cartographies designed according to the standards of the Geographic Information System (GIS) may contain additional information about the building while we assume that no 3D data of the building are available;
- 2) two aerial-photographs for stereoscopic 3D estimations (named left and right views). We assume that the views have already been corrected for internal distortions and for horectification using the external parameters. The source pictures are usually shot by an airplane and their quality requires a very high digital resolution (about 15 cm/pixel).

The flow diagram of the interactive processing consists of three steps (Fig. 1). First the cartographic map and the two aerial-photographs are aligned so that building units can be interactively or automatically selected and validated, according to pre-assigned parameters.

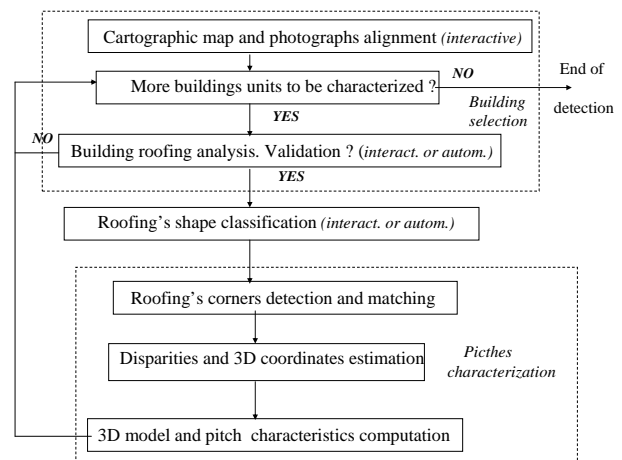


Figure 1 – Flow diagram of 3D roof modelling

The second step, also interactive or automatic, classifies the roofing shape and gives a first approximation of the available roofing areas.

The last step detects and matches the roofing corners (edges, gutters and roof tops or sheds) for exact disparity and 3D coordinates measurements. Corner detection is interactive or automatic, depending on the photographs quality. The roofing characteristics are computed using the 3D building model and stored to be used as input data to standard software programs for the estimation of the solar potential.

2. DATA ALIGNMENT AND BUILDING SELECTION

The alignment of the cartographic map with each view is an affine transform, it uses 4 markers and it is done under the supervision of a cartographic expert. The results are two views each one with the superposition of the cartographic map.

At this point there are two options: the operator can select a specific building or the building list of the cartographic map is automatically scanned (Fig. 2a). Two expanded views are generated for each validated building for further processing (Fig. 2b is a left view).

The validation can be based on different options as building ground floor area imprint, shape, etc. A Building's Record (BR) is then automatically generated to store the building parameters extracted from the cartographic map files as imprint area, main orientation, etc.

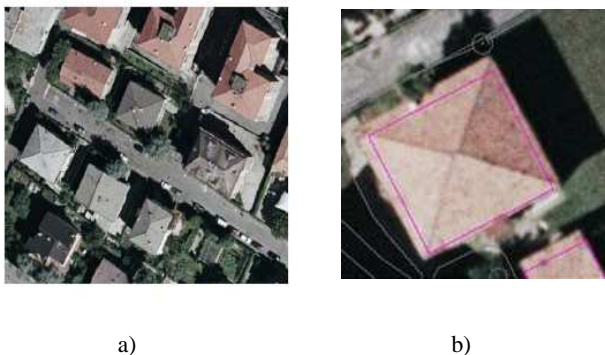


Figure 2 – a) scanned view, b) building alignment

3. BUILDING ROOFING RECOGNITION

The next step is the recognition of the roofing shape: we have defined a set of elementary roofing shapes (all with rectangular floor imprint): Flat horizontal, Barrel shaped, Sloped with one two, three or four pitches (Fig. 3); complex building roofing are interactively decomposed into the elementary shapes.

The roofing shapes are recognized according to their outlines and inner edges, moreover their colours and shadows can give useful information also about the roofing material.

The ground floor imprint of the building is used as a reference for the exact positioning of the boundary contours. Roof-

ing contours and sheds are extracted from the local enlarged images using the Canny-Deriche, thresholding and noise filtering algorithms. Edge detection is necessary also for roofing inclusions: chimneys, dormer windows, roof lights, etc. (Fig.4a).

Hough Transform (HT) is then applied to the binary edge image, its histogram in the (ρ, θ) plane (known also as Pitch HT) can be directly used for the roofing classification. The number and position of its maxima characterize the roofing shape (Fig. 4b)) that can be classified by a lookup table. A more sophisticated classifier can be implemented by a Multi Layer Perceptron (MLP) whose input are the coordinates of the maxima of the quantised Pitch HT histogram. The luminance or colour changes or histogram are necessary for the recognition of specific shapes as the Barrel ones.

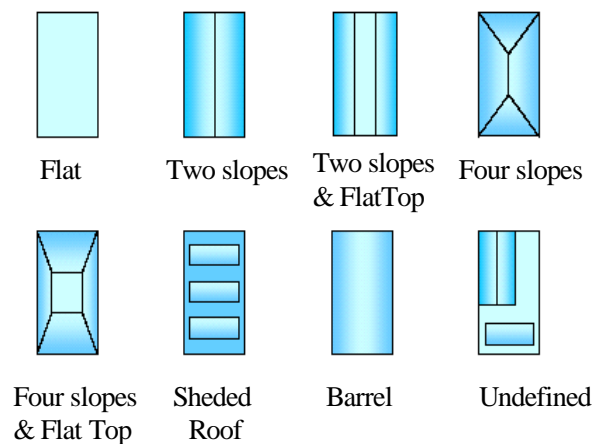


Figure 3 – Elementary Roofing Shapes [1]

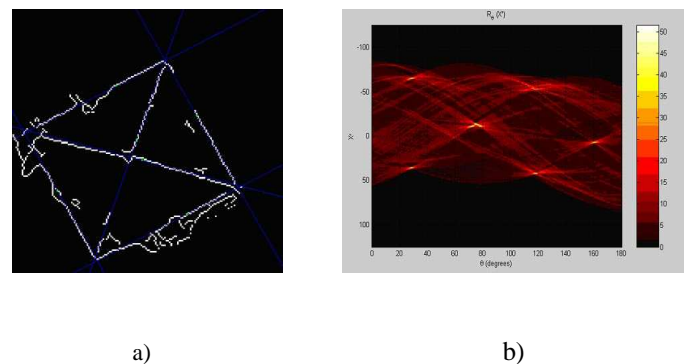


Figure 4 – a) detected contours, b) their Hough Transform

The areas of the horizontal projections of each pitch are computed using region growing limited by its contours and the detected inclusions. The recognition stage ends with an approximated evaluation of the pitches areas based on the fact that pitches slope in a geographical region is a standard: in Italy about 25° .

In the case of complex building imprint shapes interactive classification is always suggested.

4. DISPARITY AND 3D MODELLING ESTIMATION

Precise building height and pitch slopes estimation require an exact 3D model; this is possible by applying the methods of stereovision by measuring the disparity of homologous corner markers on the two stereoscopic views, along epipolar lines, and then using well known stereoscopy expressions. Marker definition, detection and selection are the preliminary steps of 3D modelling. Markers have to be easily recognisable features of the views as corners, edges, manufacts, etc. and are detected by local image analysis. Disparity measurements on epipolar lines require one-dimensional markers, they are simpler but measurements have to be executed on each epipolar line and the results need to be filtered to obtain reliable 3D results [4].

Disparity measurements on the stereoscopic views require two dimensional markers, they are more complex but the results have a better reliability.

The two methods trade off differently complexity and reliability and are being experimented and evaluated.

4.1. Profile estimation using a double projection algorithm

The markers of the corresponding epipolar lines are luminance or chrominance edges Their attributes are represented by an Attributes Vector (AV) and the difference of the AVs of a pair of homologous markers should be small with respect to that of not homologous markers pairs; the AVs have, therefore, to be rich in significant information. At present we use two components AVs: the luminance $l(i)$ and the sign of its derivative $s(i)$ at pixel i along one epipolar line.

We propose a dedicated Artificial Neural Network (ANN) [5] with a two dimensional processing layers whose nodes $P_{i,j}$ have a resonant activity function. The nodes, i and j , of the two input layers (one for each epipolar line) receive the AVs of corresponding epipolar line; their activity is transferred to the processing nodes $P_{i,j}$ (Fig.5).

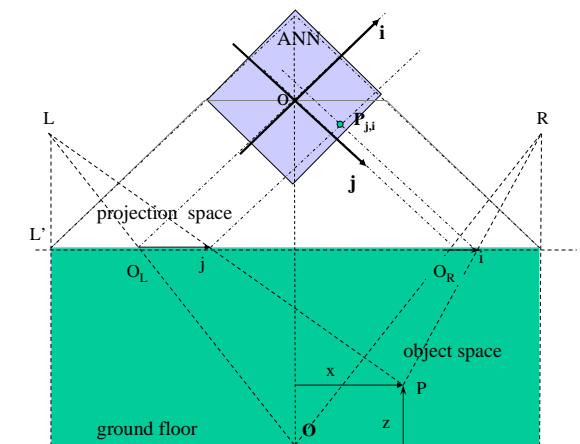


Fig.5 – Projection of the Object space into a ANN

The activity $y(i,j)$ of the processing nodes $P_{i,j}$ is:

$$y(i, j) = e^{-\alpha \cdot |l(i) - l(j)|} \cdot u[s(i) \cdot s(j)]$$

where α is a coefficient proportional to the signal-to-noise ratio of the image signal and $u[.]$ is the step function; this is necessary to select markers with the same derivative signs.

The nodes whose filtered activity is above a predefined threshold allow the detection of position of the corresponding markers in the object space:

$$x = \frac{j-1}{i+j+2 \cdot j_0}; \quad x = \frac{j+i}{i+j+2 \cdot j_0}$$

where j_0 is the distance $L'O_L = R'O_R$ measured in pixel.

By scanning all the epipolar lines we obtain the 3D model of the roofing.

Current experiments have been performed on synthetic profiles with satisfactory results and we are now starting with natural views.

4.2. Performance of different methods for disparity computation

Aim of this preliminary work is the attempt to establish a limit on the measurement accuracy of elevation differences, between eaves and roof summit, experimentally.

The measurement procedure is as follows: for each building under examination a Characteristic Point (CP) is identified which is taken as a reference level ($Z_G = 0 m$) for all the other elevation measurements. From a practical point of view, this condition is obtained by resetting the disparity of that point in the couple of stereo images. Then, elevation measurements of other structures are obtained by directly measuring their residual disparity.

In order to estimate the accuracy limit for these measurements we took into account particularly favourable structures of the roof and tried to exploit the whole informative content of the images useful to their localization.

As CPs we took roof corners and their position is obtained as intersection of the two straight lines interpolating the eaves points which compose the two corner sides. For instance, CP S_2 is obtained as intersection of segments G_1 and G_2 in Fig. 7. A segment G_i is obtained by a gradient weighted least-squares fitting (GWLS) of the contour points with a straight line.

The algorithm described in [7] was used as contours detection in the most appropriate scale ($\sigma=2$); it allows a sub-pixel resolution of $1/10$ pixel.

Experimental measurements were performed on a building with a complex geometry which is shown in Fig. 6 and are described in the following:

1. extraction of the characteristic points S_i , with $i = 1, \dots, 12$ (see Fig. 7) and evaluation of the repeatability in their localization as a function of different contour points involved in the calculation of the interpolating lines G_i .

2. Perspective recovery of the first right image R to minimize the disparity among the points S_i in R and the homologous ones in L (left image) [8]. Residual errors supply an indication on the measurement accuracy since points S_i should have the same height (same disparity) by building design and construction.
3. Taken one S_i as a reference point in the left image (S_1 in Fig. 7), the residual disparity among segments C_i ($i= 1, \dots, 5$), was measured (see Table 1). Three methods were compared. The first one computes disparities directly on the extracted segments C_i of the top of the roof. This is possible because C_i are assumed to be composed by points at the same height. An accurate estimate of their position has been obtained by interpolating the contour points with a straight line using GWLS. The second method makes use of cross correlation among a rectangular region built around the selected segment C_i in L and the right image R (Fig. 8). The last method takes into account the residual disparity of a single characteristic point K_i on the top of the roof. Point K_i is obtained as intersection of the interpolating lines of the roof edges (see Fig. 9).
4. Finally, given the residual disparity d between structures of interest, their elevation Z is computed as $Z = fB / d$, where B is the baseline and f the focal length of the stereo couple.

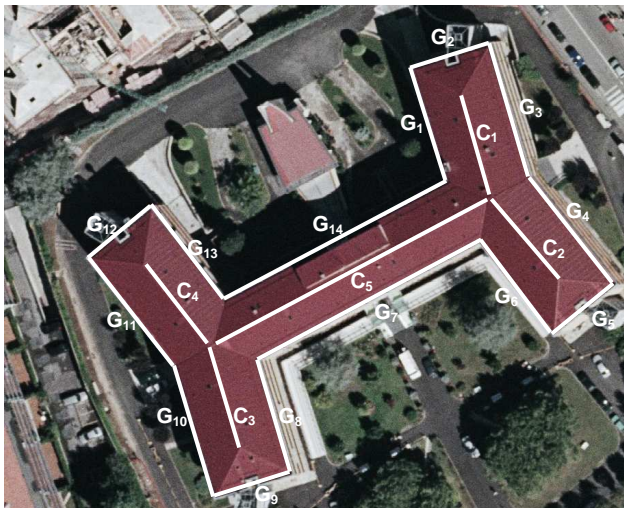


Figure 6 – Left image of the building on which the measures have been performed

From these preliminary results we can make the following considerations.

The repeatability in the characteristic points localization is very good (< 0.1 pixels) and its influence on the other measurements is negligible. These performances are justified by the fact that the image of an eaves is generally well contrasted because it is produced by physical surfaces with sharp edges.

As a consequence of the above observation, and with the hypothesis that all points S_i are at the same height, the residual error from the perspective recovery of image R can be considered as a limit for all the other measurements. In the present case we get a mean residual error of 0.26 pixels (\sim

0.3 m in Z) that can be considered acceptable for the purposes of the present project.

Analysing the results in Table 1, concerning the disparity measurement on C_i by different methods (line fitting, correlation and lines intersection), we can see a good repeatability for each measure. But there is a great lack of coherence among different measures, especially in the case of the line interpolation and correlation approaches. Indeed it is evident from the image in Fig. 6 that C_1, C_2, C_3 e C_4 should be at the same level, while C_5 is at a lower level. This means that the image processing techniques used are accurate enough but they do not consider the physical phenomena of the image forming process. Trying to justify this fact we observe that the luminance of a scene depends on the framing geometry and on the reflectance properties of surfaces. In the specific case of roof summits with rounded edges, luminances (and contour positions) can significantly change as a function of sight and illuminating angles. It must be noticed that the couples C_1, C_3 and C_2, C_4 have similar results in Table 1, first column, and similar orientations. On the other hand cross correlation should work better since it considers an extended surface of the roof. Nevertheless, a poor coherence is observed because of small information content (see Fig. 8). Figure 7 – The characteristic points detected in Fig. 6 and their reference system centred on S_1

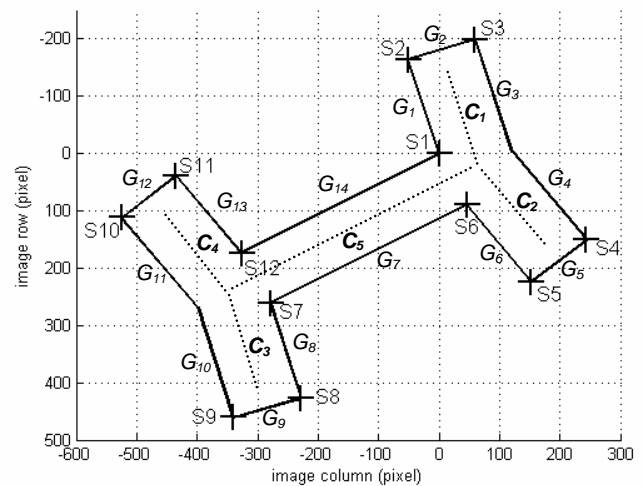
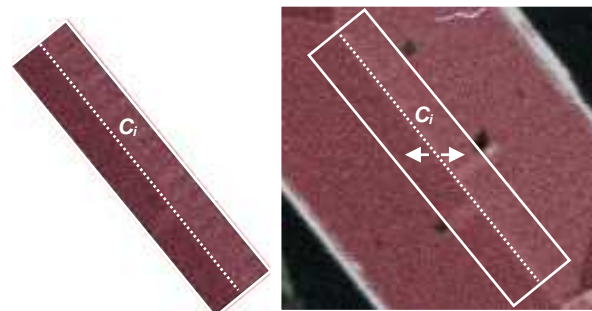


Figure 8 – The two rectangular regions built around the selected



segment C_i in the left image and the right image

Concerning the last method based on segment intersection we observe a greater coherence, and this can be explained by a greater insensitivity of this geometric feature against luminance changes. An additional evaluation of the potential performances of these methods can be derived by a theoretical analysis of an ideal system working under the present test conditions: baseline $B = 700\text{ m}$, acquisition height $H = 3000\text{ m}$, pixel pitch $P = 0.14\text{ m}$. In this case, the vertical resolution r_z is given by the relationship $r_z = (H / B) \cdot P$, that is $r_z \approx 4 \cdot P$. This means a typical resolution in Z of about 0.6 m which agrees with the accuracy in the measure of planarity.

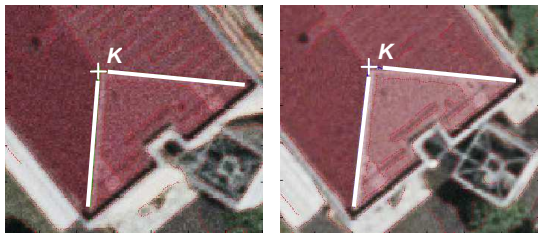


Figure 9 - The intersection point K of the straight interpolating lines of the roof edges in the two images

method	line fitting	correlation	lines intersection
disparity	$d \pm \delta d$ [pixel]		
C_1	-2.09 \pm 0.00	-1.31 \pm 0.01	-2.52 \pm 0.02
C_2	0.94 \pm 0.04	-0.19 \pm 0.56	-2.14 \pm 0.06
C_3	-2.02 \pm 0.04	-2.24 \pm 0.04	-2.21 \pm 0.09
C_4	-0.43 \pm 0.03	-1.21 \pm 0.03	-1.09 \pm 0.04
C_5	-1.91 \pm 0.06	-1.60 \pm 0.07	-1.34 \pm 0.11

Table 1 - Residual disparity d of the top of the roof and its repeatability δd computed as standard deviation over 8 measurements

5. CONCLUSIONS

The paper has presented an applied research aimed at the interactive construction of 3D building model; the work is in progress a we can give only first results.

Automatic Building roofs shape classification using the Pitch Hough Transform is quite promising for simple imprint shapes.

Concerning the construction of the profiles on epipolar lines an architecture based on two dimensional ANN has given satisfactory results on views with high signal-to-noise ratio

and it requires further improvement in marker selection to become really reliable.

Concerning the last approach (disparity computation), possible improvements could be obtained by using a more sophisticated model of the image forming process and by exploiting more favourable illuminating conditions to enhance surface contrasts.

Moreover the proposed system has to be validated with a recent software Gcarto of Geosoft that has to be used by an expert while our aim is a system to be operated by unskilled operators.

The major motivations of the research are being met when a large number of buildings of a medium sized town, in the order of a few hundreds, has to be analysed for estimating the actual local solar energy potential.

Acknowledgments

The authors thanks the cooperation of the Master students: Andrea Castelli, Marco Codazzi and Lucia Pezzuto.

References

[1] NET Novak « Le Potentiel Solaire dans le Canton de Genève-Analyse et Evaluation du Potentiel Solaire- Photovoltaïque et Thermique -dans le Parc Immobilier Public du Canton de Genève » ;*Rapport Technique November 2004 ,NET Nowak Energie & Technologie SA Waldweg 8 CH-1717 St. Ursen.*

[2] <http://re.jrc.cec.eu.int/pvgis/pvestframe.php?en&euope>

[3] K. Ulm: “ 3D City Models from Aerial Imaginery- Integrating Images and the Landscape” in *GEOInformatics Jan/Feb 2005, Volume 8, February 2005.*

[4] C. Baillard : « Analyse d'images aériennes stéréoscopiques pour la restitution 3-D des milieux urbains », thèse de doctorat de ENST, 10 octobre 1997.

[5] R.D. Henkel : " A Fast parallel Algorithm for Stereovision " 0-8186-7987-5/97, 1997 IEEE.

[6] H. Jibrini : "Reconstruction automatique de bâtiments en modèles polyédriques 3-D à partir de données cadastrales vectorisées 2D et d'un couple d'images aériennes à haute résolution", *Thèse de Doctorat ENTS (2002)* .

[7] P. Grattoni, A. Guiducci: "Contour coding for image description" in *Pattern Recognition Letters*, Vol. 11(2), pp. 95-105, 1990.

[8] R. Hartley and A. Zisserman "Multiple View Geometry in Computer Vision", Cambridge University Press, June 2000.